



ISSN: 2230-9926

Available online at <http://www.journalijdr.com>

IJDR

International Journal of Development Research

Vol. 13, Issue, 03, pp. 61935-61944, March, 2023

<https://doi.org/10.37118/ijdr.26371.03.2023>



RESEARCH ARTICLE

OPEN ACCESS

MIXED CONVECTION BOUNDARY LAYER NANOFUID FLOW OVER AN INCLINED STRETCHING CYLINDER WITH THERMAL RADIATION

*Jarwal, V. K., Choudhary, S. and Sinha, S.

Department of Mathematics, University of Rajasthan, Jaipur-302004, Rajasthan, India

ARTICLE INFO

Article History:

Received 28th January, 2023

Received in revised form

09th February, 2023

Accepted 23rd February, 2023

Published online 28th March, 2023

KeyWords:

Nanofluid; MHD flow; Thermal radiation; Stretching cylinder; Porous medium.

*Corresponding author: Jarwal, V. K.,

ABSTRACT

Lecturers Present article classifies the influence of mixed convection boundary layer *MHD* flow of nanofluid (*Ag/ Cu-H₂O*) through porous stretching cylinder in the presence of thermal radiation. The governing non-linear *PDE*'s are reduced to *ODE*'s with boundary conditions by using similarity transformations. The numerical method known as Runge – Kutta fourth order has been taken in to account with shooting technique to solve the obtained *ODE*'s with assisting boundary conditions. The impact of thermal radiation parameter on Nusselt number along with mixed convection parameter and heat generation/absorption parameter are shown by graphical and tabular way. The outcome showed that Nusselt number decreases with an increase in radiation absorption parameter and heat generation/absorption parameter while reverse result obtained for mixed convection parameter. The comparison of our data with published one has admirable result.

Copyright©2023, Jarwal et al. This is an open access article distributed under the Creative Commons Attribution License, which permits unrestricted use, distribution, and reproduction in any medium, provided the original work is properly cited.

Citation: Jarwal, V. K., Choudhary, S. and Sinha, S. 2023. "Mixed convection boundary layer nanofluid flow over an inclined stretching cylinder with thermal radiation", *International Journal of Development Research*, 13, (03), 61935-61944.

INTRODUCTION

Nanofluid is mix suspension of nanometer sized solid particles (*Cu, Al, Ag*, etc.) in base fluid such as water, oil and ethylene glycol, which is first introduced by Choi [4]. Due to the fact that thermal conductivity of the nanoparticles is larger than regular fluids, the term nanofluid has become an interesting topic for the researchers in last few decades. There are several manufacturing and technology applications of nanofluids such as engine cooling, refrigerator, microelectronics, cancer therapy, drug delivery and glues. Heat transfer also uses in various industrial areas such as fuel cells, microelectronics, pasteurization of food and biomedical/ pharmaceutical processes. The steady flow of fluid past over a stretching cylindrical surface was introduced by Wang [27]. Incompressible and laminar viscous fluid flow caused by stretching cylinder was scrutinized by Ishak and Nazar [12]. There are several utilizations of convective flow in a porous medium such as building erection, solar collectors, ventilation procedure and removal of heat from nuclear reactors. Pal et al. [22] have conferred the effect of thermal radiation on nanofluid flow with porous medium due to stretching/shrinking sheet. Ishak et al. [11] studied the impact of suction/injection on fluid motion and heat transfer towards permeable stretching cylinder. The combined effect of thermal conductivity and dynamic viscosity with the existence of stretching permeable tube in nanofluid was described by Ahmed et al. [1].

The concept of magnetohydrodynamics (*MHD*) is very important in devices with high thermal properties like in physiological equipment involving blood pumping machines, *MRI*, hyperthermia and flow in arteries. Ashorynejad et al. [2] have studied the impact of *MHD* flow over a stretching cylinder within nanofluid. Majeed et al. [14] have scrutinized the mixed influence of partial slip and heat transfer on steady non-Newtonian Casson fluid flow along stretchable cylinder with arranged heat flux. The analytical results of magnetohydrodynamic (*MHD*) third grade fluid flow over a stretching cylinder were computed by Hayat et al. [8]. Butt et al. [3] investigated the magnetic field effects on entropy generation and viscous flow over a stretching cylinder embedded in a porous medium. "Combined effects of viscous dissipation and Joule heating on *MHD* Sisko nanofluid over a stretching cylinder" was investigated by Hussain et al. [10]. Naramgari and Sulochana [21] investigated on "*MHD* flow of dusty nanofluid over a stretching surface with volume fraction of dust particles". Mukhopadhyay [20] proposed *MHD* boundary layer slip flow towards a stretching cylinder. Pandey and Kumar ([23], [25]) have analyzed the boundary layer flow and heat transfer of nanofluid over stretching cylinder with different effects. Malik et al. [15] studied the Cattaneo-Christov heat flux model for Sisko fluid flow via nonlinear stretching cylinder. Ohmic-viscous dissipation and heat generation/absorption with magnetic field effect on *Cu*-water nanofluid flow through stretching/shrinking channel was analyzed by Pandey and Kumar [24].

Ganga *et al.* [5] considered “MHD radiative boundary layer flow of nanofluid past a vertical plate with internal heat generation/absorption, viscous and ohmic dissipation effects”. Sisko nanofluid flow over a stretching surface was analyzed by Khan *et al.* [13] using both analytical and numerical methods in the presence of convective boundary conditions. Second order slip flow of nanofluid over a stretching/shrinking sheet with thermal radiation and magnetic field effect was studied by Hakeem *et al.* [6]. Hayat *et al.* [7] evaluated the role of Joule heating and melting heat transfer in the MHD flow of Cu-water nanofluid flow. The influence of Joule heating on MHD tangent hyperbolic peristaltic nanofluid flow through inclined channel with slip conditions was observed by Hayat *et al.* [9]. Singh *et al.* [26] discussed the non-uniform heat source effects along with melting heat transfer on magnetic Cu-water nanofluid flow via porous cylinder. Mishra *et al.* ([16]- [19]) examined several effects on MHD Ag-water nanofluid flow utilizing different geometries. In view of above literature survey and development of research in nanofluids, it is revealed that mixed convection Ag-water and Cu-water nanofluid flow through an inclined porous stretching cylinder with thermal radiation has not been studied yet, therefore the intention of present research is to investigate this aforesaid problem. The governing boundary layer equations are simplified using similarity variables which are then solved numerically using Runge- Kutta fourth order method with shooting technique. The influence of various parameters on heat transfer characteristics and the flow field are explored and depicted through graphs or tables.

Nomenclature

B_0	Magnetic field strength ($\text{m t}^2\text{A}^{-1}$)	u_w	Suction velocity (m/s)
C_p	Specific heat at constant pressure (J/kg K)	u, w	Velocity component along r - and z - direction (m/s)
C_f	Skin friction coefficient	z, r	Cylindrical coordinates (m)
D	Local mixed convection parameter		
Ec	Eckert number		<i>Greek symbols</i>
f	Dimensionless stream function	α	Thermal diffusivity (m^2/s)
g	Acceleration due to gravity (m/s^2)	β	Thermal expansion coefficient (K^{-1})
Ha^2	Magnetic field parameter	γ	Angle of inclination of cylinder
K_0	Permeability of the porous medium (m^2)	\mathcal{K}	Thermal conductivity (m^2/s)
K	Permeability parameter	μ	Dynamic viscosity (Kg/ms)
l_1	Velocity slip factor (m)	ρ	Density (kg/m^3)
l_2	Thermal slip factor (m)	σ	Electric conductivity ($\text{Kg}^{-1}\text{m}^{-3}\text{t}^3\text{A}^2$)
Nu	Nusselt number	ν	Kinematic viscosity (m^2/s)
Pr	Prandtl number	λ	Velocity slip parameter
Q_0	Heat generation/absorption coefficient ($\text{W/m}^2\text{K}$)	θ	Dimensionless temperature
Q	Heat generation/absorption parameter	δ	Thermal slip parameter
R	Radiation absorption parameter	ϕ	volume fraction of nanoparticles
Re	Reynolds number	η	Similarity variable
S	Suction/injection parameter		<i>Subscript</i>
T	Temperature of the nanofluid (K)	f	Base fluid
T_w	Wall temperature (K)	S	Nanoparticle
T_∞	Ambient temperature (K)	nf	Nanofluid

Mathematical Formulation

We have considered an axisymmetric, incompressible, steady, laminar flow of a nanofluid over a porous inclined stretching cylinder with diameter $2a$. z -axis and r -axis are considered in horizontal and vertical direction of the cylinder, respectively as signified in Fig. 1. Towards radial direction we assume that intensity of uniform magnetic field is B_0 . Along z -direction, the cylinder is being stretched with velocity $W_w = 2cz$, where c is stretching rate. We also assume that T_w is the surface temperature of the cylinder and ambient fluid temperature is T_∞ , where ($T_w > T_\infty$). The regular fluid (water) based nanofluid containing Ag (silver) or Cu (copper) as nanoparticles is considered. The physical properties of regular fluid and nano particles are depicted in Table 1. Under the all above postulations, the boundary-layer equations are articulated as follows (Ahmed *et al.* [1], Ashorynejad *et al.* [2] and Ishak *et al.* [11]):

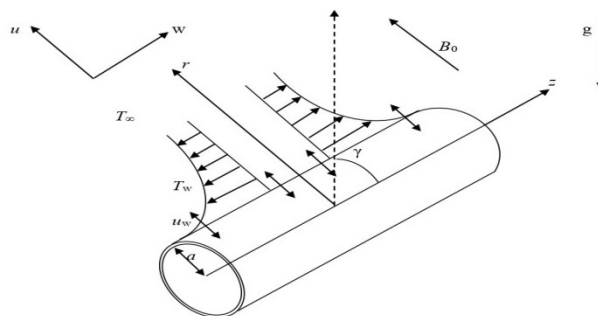


Fig. 1. Physical sketch and the coordinate system

$$\frac{\partial(rw)}{\partial z} + \frac{\partial(ru)}{\partial r} = 0, \quad (1)$$

$$\rho_{nf} \left(w \frac{\partial w}{\partial z} + u \frac{\partial w}{\partial r} \right) = \mu_{nf} \left(\frac{\partial^2 w}{\partial r^2} + \frac{1}{r} \frac{\partial w}{\partial r} \right) - \sigma_{nf} B_0^2 w - \frac{\mu_{nf} w}{K_0} + g(\rho\beta)_{nf} (T - T_\infty) \cos \gamma, \quad (2)$$

$$(\rho C_p)_{nf} \left(w \frac{\partial T}{\partial z} + u \frac{\partial T}{\partial r} \right) = \kappa_{nf} \left(\frac{\partial^2 T}{\partial r^2} + \frac{1}{r} \frac{\partial T}{\partial r} \right) + \sigma_{nf} B_0^2 w^2 + \mu_{nf} \left(\frac{\partial w}{\partial r} \right)^2 + Q_0 (T - T_\infty) - \frac{\partial q_r}{\partial r}, \quad (3)$$

Corresponding boundary conditions for the model are as follows (Mishra and Kumar [16]):

$$u = u_w, w = W_w + l_1 \frac{\partial w}{\partial r}, T = T_w + l_2 \frac{\partial T}{\partial r} \quad \text{at } r = a;$$

$$u \rightarrow 0, T \rightarrow T_\infty \quad \text{as } r \rightarrow \infty, \quad (4)$$

where velocity slip factor and thermal slip factor are l_1 and l_2 , respectively.

The effective density ρ_{nf} , heat capacitance $(\rho C_p)_{nf}$, dynamic viscosity μ_{nf} , thermal conductivity κ_{nf} and electric conductivity σ_{nf} of nanofluid are described as (Ashorynejad *et al.* [2] and Singh *et al.* [26]):

$$(\rho\beta)_{nf} = (1-\phi)(\rho\beta)_f + \phi(\rho\beta)_s$$

$$\rho_{nf} = (1-\phi)\rho_f + \phi\rho_s, (\rho C_p)_{nf} = (1-\phi)(\rho C_p)_f + \phi(\rho C_p)_s,$$

$$\frac{\mu_{nf}}{\mu_f} = \frac{1}{(1-\phi)^{2.5}}, \frac{\kappa_{nf}}{\kappa_f} = \frac{\kappa_s + 2\kappa_f - 2\phi(\kappa_f - \kappa_s)}{\kappa_s + 2\kappa_f + \phi(\kappa_f - \kappa_s)}, \frac{\sigma_{nf}}{\sigma_f} = (1-\phi) + \phi \frac{\sigma_s}{\sigma_f}, \quad (5)$$

where volume fraction of nanoparticles is taken as ϕ .

By using Rosseland approximation, the radiative heat flux is

$$q_r = -\frac{4\sigma^*}{3k^*} \frac{\partial T^4}{\partial y}, \quad (6)$$

where k^* is the absorption coefficient, σ^* is the Stefan-Boltzman constant. The temperature difference is assuming such that T^4 may be expanded as a Taylor series about T_∞ and neglecting higher order terms, we get $T^4 \approx 4T_\infty^3 T - 3T_\infty^4$ and using it in equation (6), we get

$$q_r = -\frac{16\sigma^* T_\infty^3}{3k^*} \frac{\partial T}{\partial y} \quad \text{and hence } \frac{\partial q_r}{\partial y} = -\frac{16\sigma^* T_\infty^3}{3k^*} \frac{\partial^2 T}{\partial y^2}. \quad (7)$$

To convert the governing equations into the system of nonlinear ODE's, we introduce following similarity variables (Ahmed *et al.* [1], Ashorynejad *et al.* [2] and Ishak *et al.* [11]):

$$u = -\frac{ca}{\sqrt{\eta}} f(\eta), w = 2zc f'(\eta), \eta = \left(\frac{r}{a}\right)^2, \theta(\eta) = \frac{T - T_\infty}{T_w - T_\infty}, \quad (8)$$

Using Equations (5)-(8) into Equations (2)-(3), we acquire following system of nonlinear ODE's:

$$A_3(\eta f'''' + f''') + A_1 \text{Re}(f f'' - f'^2) - A_5 Ha^2 f' - A_3 K f' + A_6 D \cos \gamma \theta = 0, \quad (9)$$

$$A_2 \text{Re Pr } f \theta' + A_4(\eta \theta'' + \theta') + A_3 \text{Pr Ec } \eta f''^2 + \frac{A_5}{2} Ha^2 \text{Ec Pr } f'^2 + \frac{4}{3} R \eta \theta'' + Q \theta = 0, \quad (10)$$

with the association of boundary conditions in terms of f and θ :

$$f(1) = S, f'(1) = 1 + \lambda f''(1), \theta(1) = 1 + \delta \theta'(1) \quad \text{at } \eta = 1;$$

$$f'(\infty) \rightarrow 0, \theta(\infty) \rightarrow 0 \text{ as } \eta \rightarrow \infty, \quad (11)$$

where prime denotes differentiation with respect to η .

The parameters used in equations (9) to (11) are as follows:

$$\begin{aligned} \text{Pr} &= \frac{\nu_f}{\alpha_f}, \text{Re} = \frac{c a^2}{2\nu_f}, M = \frac{\sigma_f B_0^2 a^2}{2\rho_f \nu_f}, K = \frac{a^2}{2K_0}, D = \frac{\beta_f g a^2 (T_w - T_\infty)}{2W_w \nu_f}, R = \frac{4T_\infty^3 \sigma^*}{k^* \kappa_f}, \\ Q &= \frac{Q_0 a^2}{4\kappa_f}, S = -\frac{u_w}{c a}, Ec = \frac{W_w^2 \rho_f}{(\rho C_p)_f (T_w - T_\infty)}, \lambda = \frac{2l_1}{a}, \delta = \frac{2l_2}{a}, A_1 = (1-\phi) + \phi \left(\frac{\rho_s}{\rho_f} \right), \\ A_2 &= (1-\phi) + \phi \left(\frac{(\rho C_p)_s}{(\rho C_p)_f} \right), A_3 = \frac{\mu_{nf}}{\mu_f}, A_4 = \frac{\kappa_{nf}}{\kappa_f}, A_5 = \frac{\sigma_{nf}}{\sigma_f}, A_6 = (1-\phi) + \phi \left(\frac{(\rho\beta)_s}{(\rho\beta)_f} \right). \end{aligned} \quad (12)$$

Here A_1, A_2, A_3, A_4, A_5 and A_6 are constants.

Important non-dimensional physical quantities, the skin friction coefficient and the local Nusselt number can be defined respectively as follows:

$$C_f = \frac{2\mu_{nf}}{W_w^2 \rho_f} \left(\frac{\partial w}{\partial r} \right)_{r=a}, \quad Nu = -\frac{a \kappa_{nf}}{\kappa_f (T_w - T_\infty)} \left(\frac{\partial T}{\partial r} \right)_{r=a}, \quad (13)$$

Now, using Equation (4) and (8) in Equation (13), the reduced skin friction coefficient and the reduced Nusselt number are given as follows:

$$(z \text{Re}/a) C_f = A_3 f''(1), \quad Nu = -2 A_4 \theta'(1). \quad (14)$$

Numerical Method

The dimensionless momentum Equation (9) and energy Equation (10) together with associated boundary conditions (11) are solved numerically by applying Runge-Kutta fourth order method with shooting technique. In this problem, we set up the following terms into the obtained boundary layer equations to convert these equations into first-order ODE's:

$$f = f_1, f_1' = f_2, f_1'' = f_3, \theta = f_4, f_4' = f_5.$$

Using above mentioned substitutions, the following system of first-order ODE's is obtained:

$$\begin{aligned} f_1' &= f_2, \\ f_2' &= f_3, \\ f_3' &= \left(\frac{1}{\eta A_3} \right) \left[A_1 \text{Re} (f_2^2 - f_1 f_3) + A_5 Ha^2 f_2 + A_3 K f_2 - A_6 D \cos \gamma f_4 - A_3 f_3 \right], \\ f_4' &= f_5, \\ f_5' &= - \left\{ \frac{1}{\eta \left(A_4 + \frac{4R}{3} \right)} \right\} \left[A_4 f_5 + A_2 \text{Re Pr } f_1 f_5 + A_3 \eta \text{Pr } Ec f_3^2 + \frac{A_3}{2} Ha^2 Ec \text{Pr } f_2^2 + Q f_4 \right], \end{aligned}$$

with initial conditions

$$\eta = 1: f_1 = S, f_2 = 1 + \lambda f_3, f_4 = 1 + \delta f_5;$$

$$\eta \rightarrow \infty: f_2 \rightarrow 0, f_4 \rightarrow 0.$$

Using Runge-kutta fourth order method, the system of first order ODE's along with initial conditions is solved and also apply appropriate guessing for missing initial values by the shooting method for several sets of parameters until the conditions $f'(\eta \rightarrow \infty) = 0$ and $\theta(\eta \rightarrow \infty) = 0$ hold.

RESULTS AND DISCUSSION

The altered non-dimensional *ODE*'s (9) and (10) with related boundary conditions (11) are solved numerically with the aid of Runge-Kutta fourth order method via shooting technique. We select the range of affecting parameters as: $0.0 \leq K \leq 4.0$, $1.0 \leq Ha^2 \times 10^{-8} \leq 4.0$, $-2.0 \leq Q \leq 2.0$, $0.0 \leq R \leq 0.2$, $5.0 \leq Re \leq 7.0$, $0.1 \leq D \leq 5.0$, $4.0 \leq Pr \leq 10.0$, $0.0 \leq \gamma \leq \pi/2$, $0.2 \leq Ec \leq 0.6$, $-0.1 \leq S \leq 0.1$, $0.2 \leq \lambda \leq 0.4$ and $0.1 \leq \delta \leq 0.3$. Throughout the whole process of numerical analysis, the default values of parameters are considered as: $K=1.0$, $Ha^2 \times 10^{-8}=1.0$, $Ec=0.3$, $Pr=6.2$, $Q=0.5$, $D=0.1$, $S=0.1$, $Re=5.0$, $\delta=0.1$, $R=0.1$, $\phi=0.05$, $\gamma=\pi/4$ and $\lambda=0.2$ unless stated separately. In Fig. 2 and Fig. 3 consequence of permeability parameter (K) on velocity and temperature profiles are disclosed. It exhibits that velocity profile diminishes while temperature profile increases with an enhancement in the permeability parameter (K). The variations among velocity and temperature profiles for various values of magnetic field parameter (Ha^2) are sketched in Fig. 4 and Fig. 5. It is seen from Fig. 4 and Fig. 5 that for increasing value of magnetic field parameter (Ha^2), velocity of existing fluid decelerates and temperature accelerates. A force determined as the Lorentz force is always generated for an electrically conducting fluid in the presence of magnetic field. This force reduces the motion of fluid within the boundary layer region. Fig. 6 displays the effect of heat generation/absorption parameter (Q) on temperature profile and declares that temperature of nanofluid is an increasing function of Q . The impact of radiation absorption parameter (R) on temperature distribution is portrayed in Fig. 7. From this outline, it is observed that nanofluid temperature increases with the influence of R . Fig. 8 and Fig. 9 are graphed to examine the nature of velocity and temperature of nanofluid corresponding to distinct values of Reynolds number (Re). It is cleared from Fig. 8 and Fig. 9 that on accelerating the values of Reynolds number, velocity and temperature of nanofluid continuously decreases. The impact of mixed convection parameter (D) on velocity graph is shown in Fig. 10.

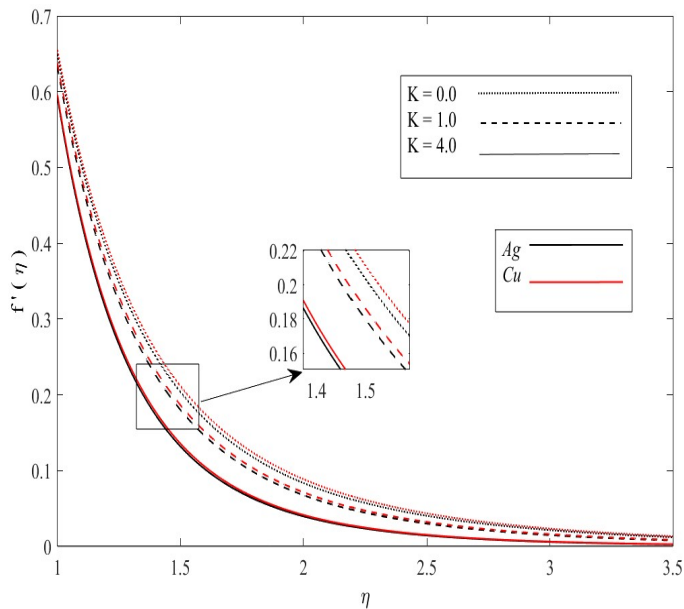


Fig. 2. Velocity behavior for various values of K

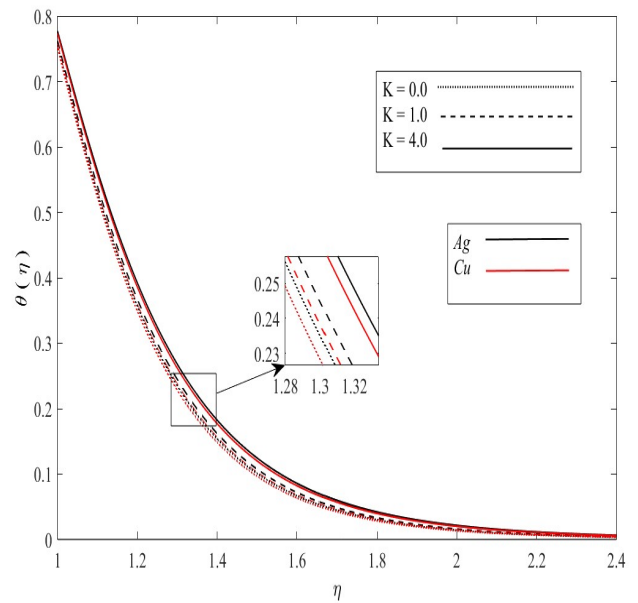


Fig. 3. Temperature behavior for various values of K

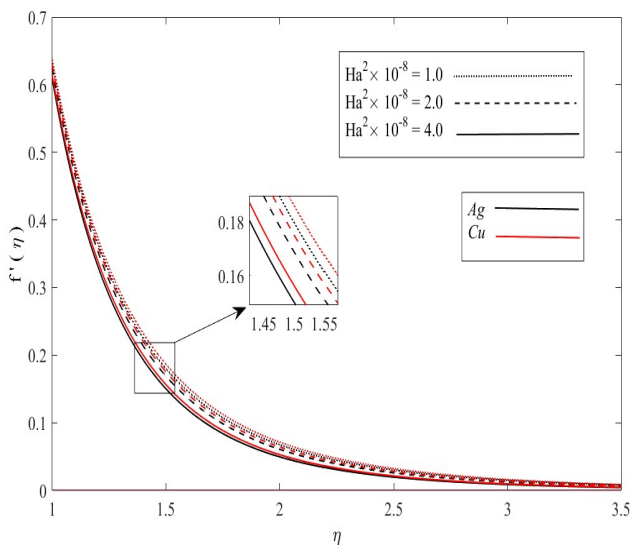


Fig. 4. Velocity behavior for various values of Ha^2

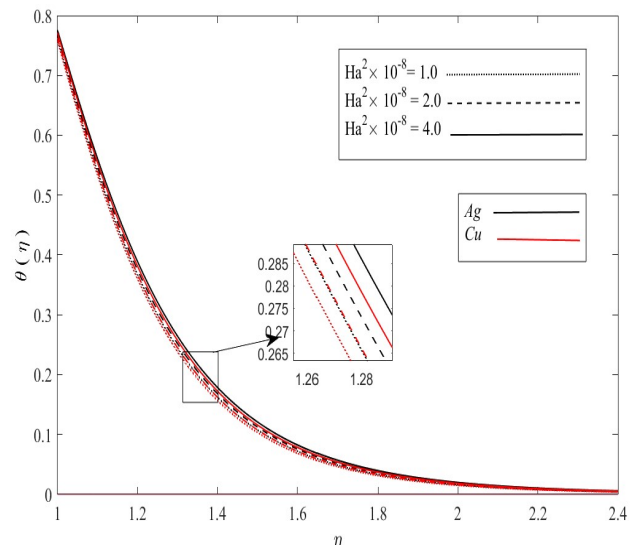


Fig. 5. Temperature behavior for various values of Ha^2

It is observed from Fig. 10 that the velocity boundary thickness of nanofluid rises up with growing values of D . The temperature distribution due to several values of Eckert number (Ec) is sketched in Fig. 11. According to this figure, nanofluid temperature accelerates due to an enhancement in Eckert number. Fig. 12 and Fig. 13 depict the velocity and temperature profiles corresponding to the suction/injection parameter (S). These curves identified that velocity and temperature of nanofluid retards as parameter S moves from injection to suction. Fig. 14 shows the influence of

velocity slip parameter (λ) on velocity profile. This graph declares that as λ increases, the velocity profile decreases. The variation in temperature profile with respect to thermal slip parameter (δ) is depicted in Fig. 15.

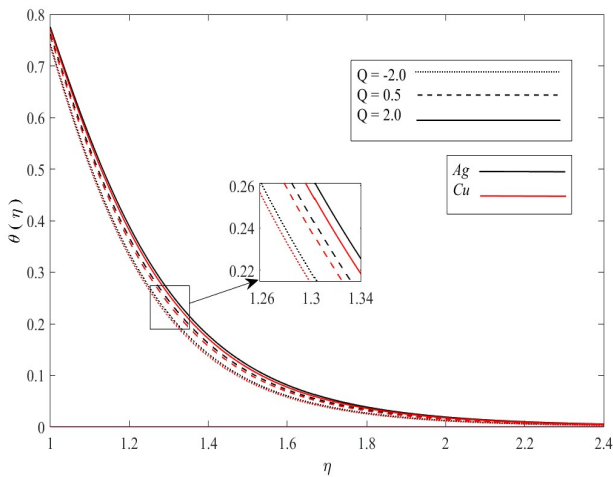


Fig. 6. Temperature behavior for various values of Q

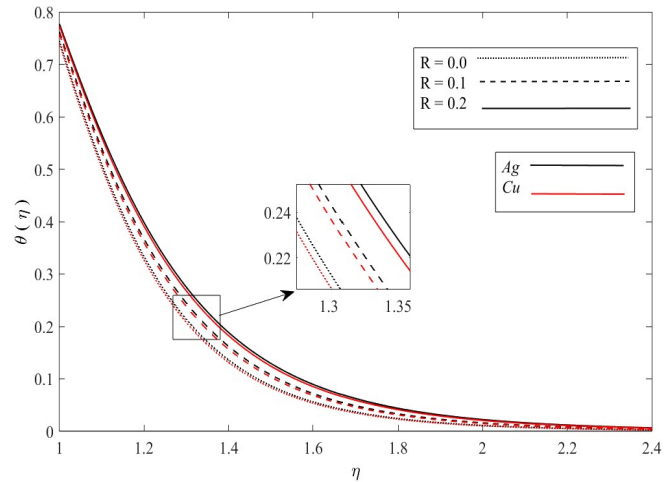


Fig. 7. Temperature behavior for various values of R

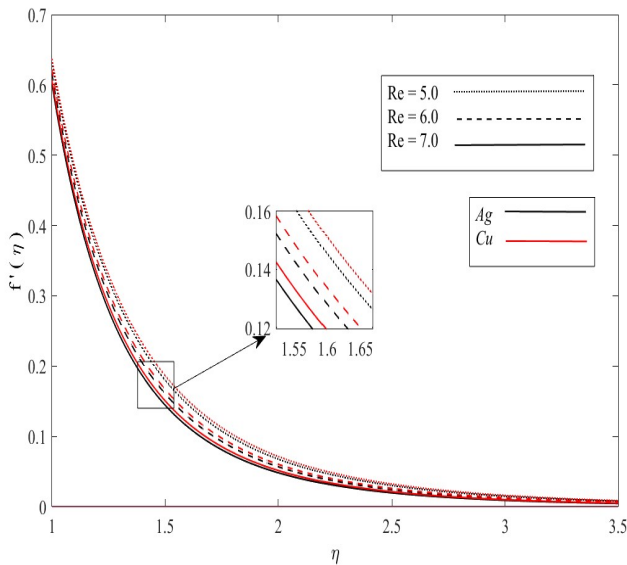


Fig. 8. Velocity behavior for various values of Re

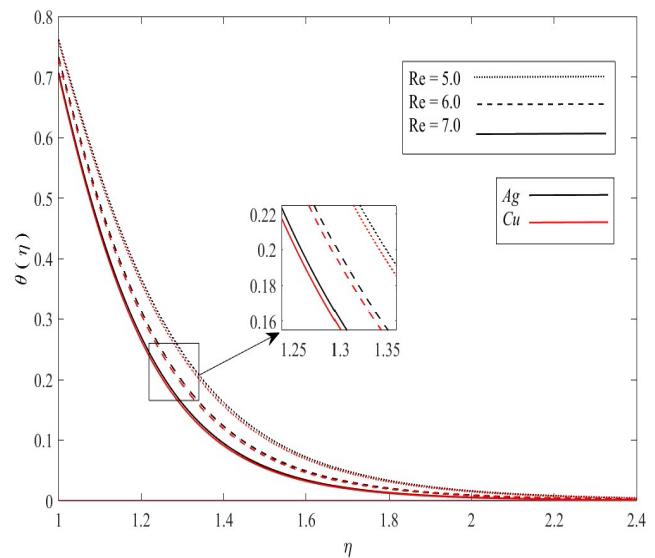


Fig. 9. Temperature behavior for various values of Re

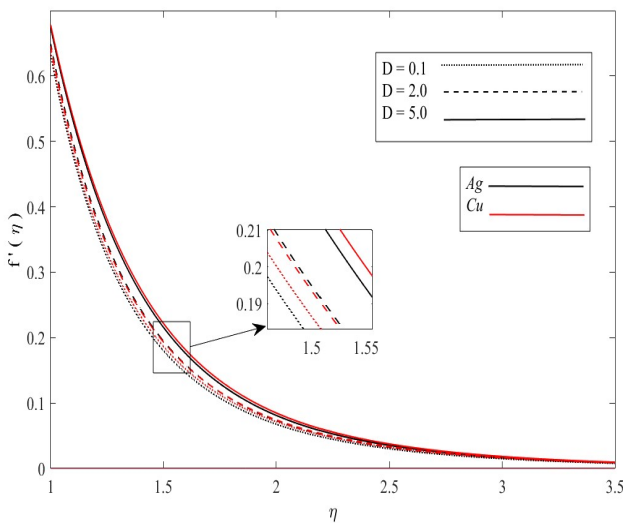


Fig. 10. Velocity behavior for various values of D .

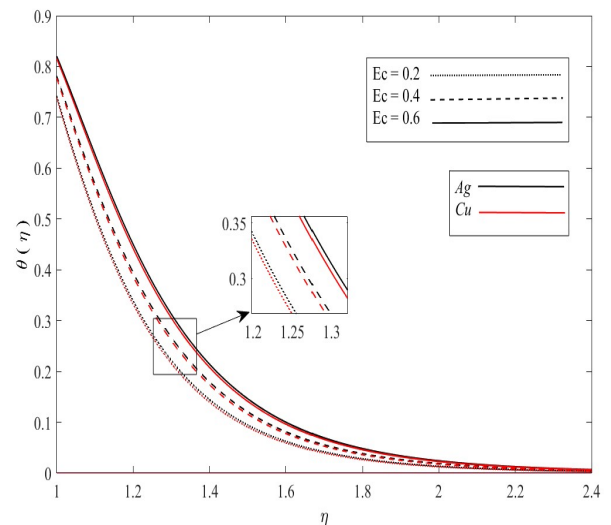


Fig. 11. Temperature behavior for various values of Ec

From this figure, it is outlined that an enhancement in δ causes decrease in temperature profile. Fig. 16 illustrates the effect of inclination angle on velocity of nanofluid. Referring to Fig. 16, we deduce that velocity of nanofluid continuously diminishes when cylinder shifts its position from vertical to horizontal. To examine the authenticity of numerical outcomes, we studied a comparison of present data with published one which is obtained by wang [27], Ahmed *et al.* [1] and Mishra and Kumar [16]. Admirable results have been detected on viewing Table 2.

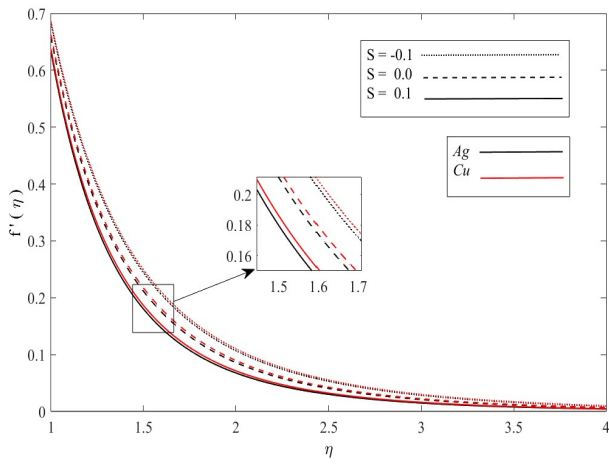


Fig. 12. Velocity behavior for various values of S

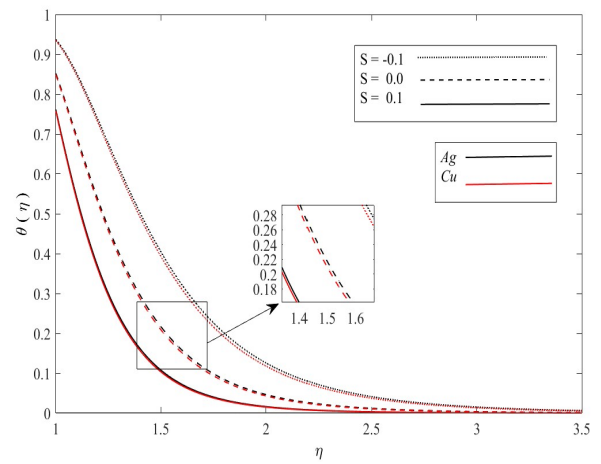


Fig. 13. Temperature behavior for various values of S

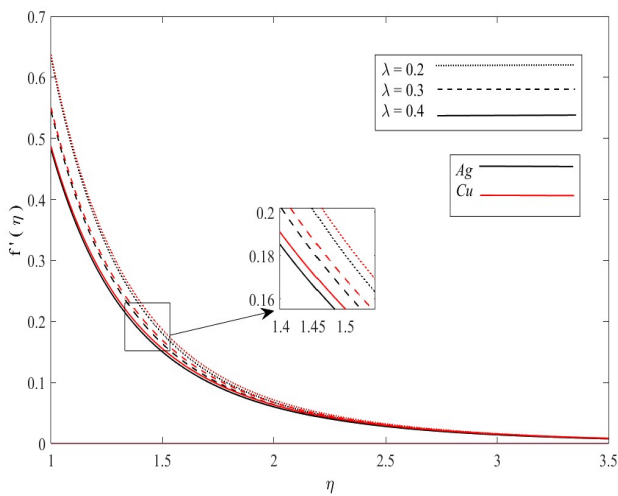


Fig. 14. Velocity behavior for various values of λ

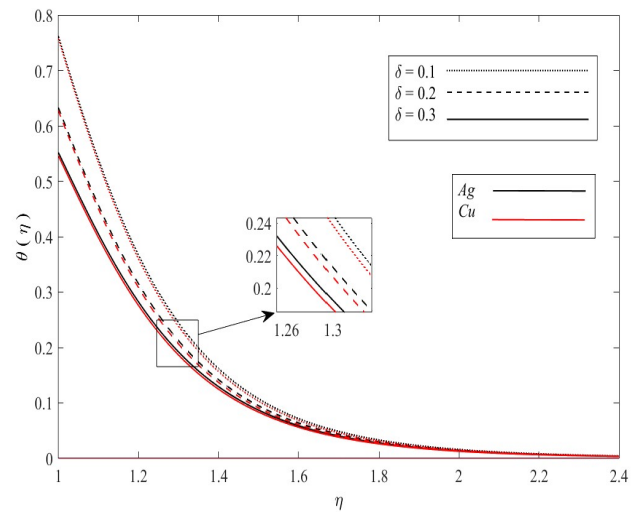


Fig. 15. Temperature behavior for various values of δ

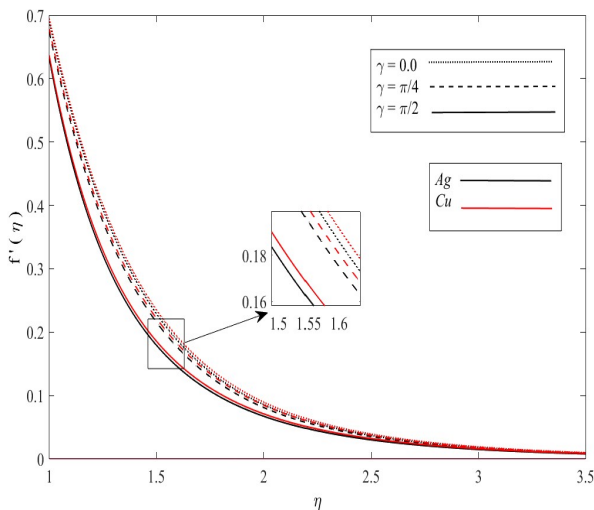


Fig. 16. Velocity behavior for various values of γ when $D=5.0$

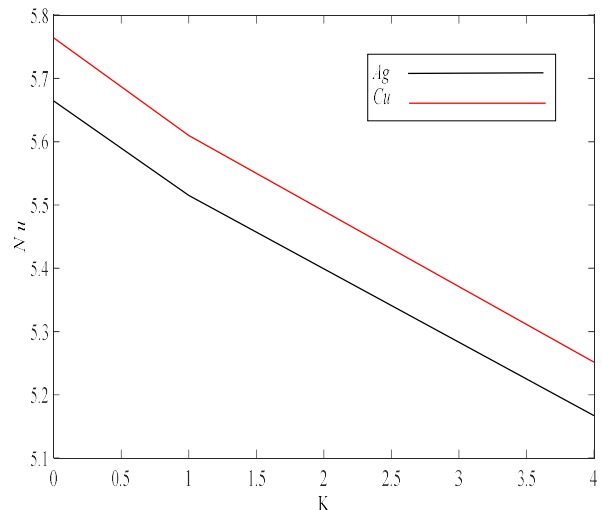


Fig. 17. Comparison of Nusselt number for $Ag-H_2O$ and $Cu-H_2O$ nanofluid w. r. t. K .

Table 1. Thermophysical properties of water and nanoparticles (Ahmed *et. al.* [1])

	ρ (kg/m ³)	C_p (J/kg K)	K (W/m K)	σ (S/m)	$\beta \times 10^{-5}$ (K ⁻¹)
Pure water	997.1	4179	0.613	0.05	21
Silver (<i>Ag</i>)	10,500	235	429	6.3×10^7	1.84
Copper (<i>Cu</i>)	8933	385	401	5.96×10^7	1.67

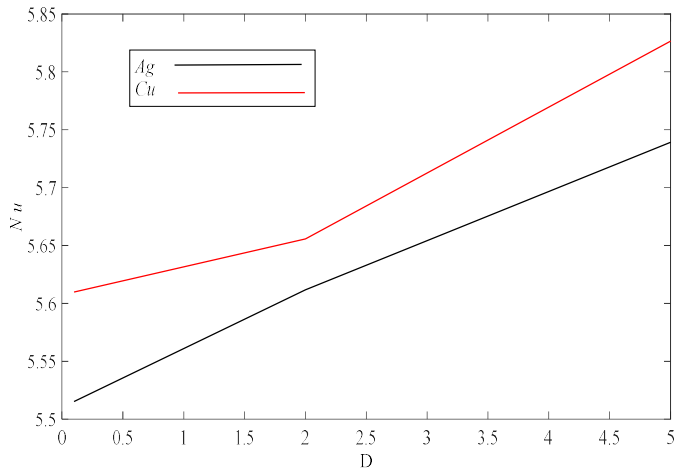


Fig. 18. Comparison of Nusselt number for Ag-H₂O and Cu-H₂O nanofluid w. r. t. D.

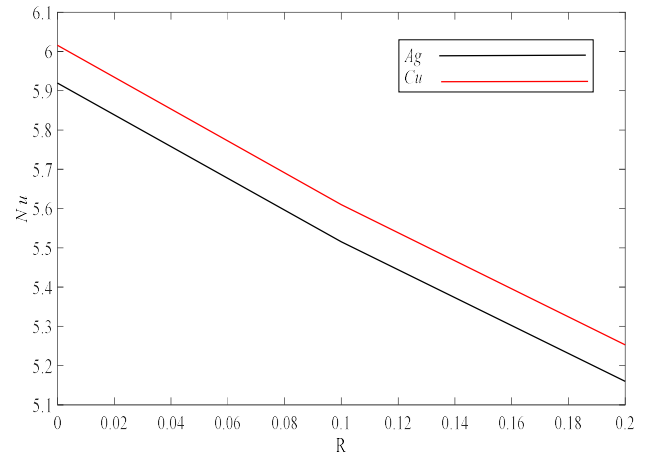


Fig.19. Comparison of Nusselt number for Ag-H₂O and Cu-H₂O nanofluid w. r. t. R.

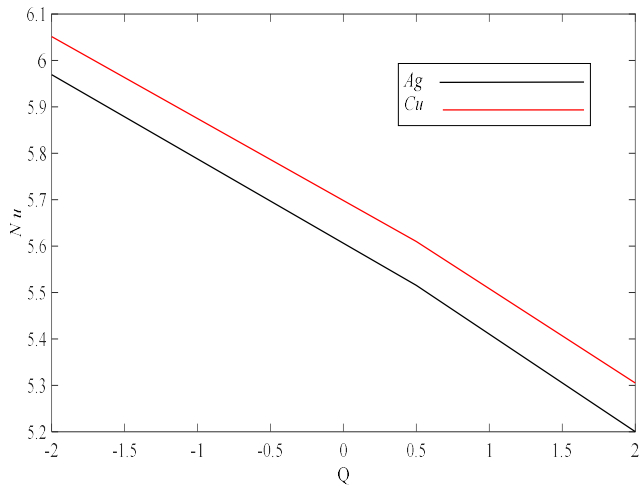


Fig. 20. Comparison of Nusselt number for Ag-H₂O and Cu-H₂O nanofluid w. r. t. Q.

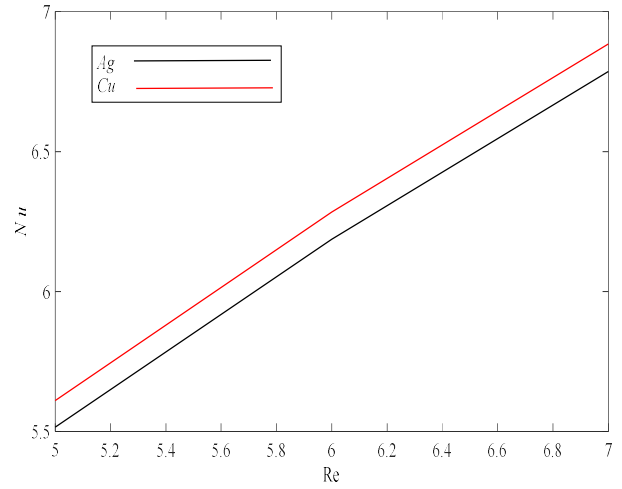


Fig. 21. Comparison of Nusselt number for Ag-H₂O and Cu-H₂O nanofluid w. r. t. Re.

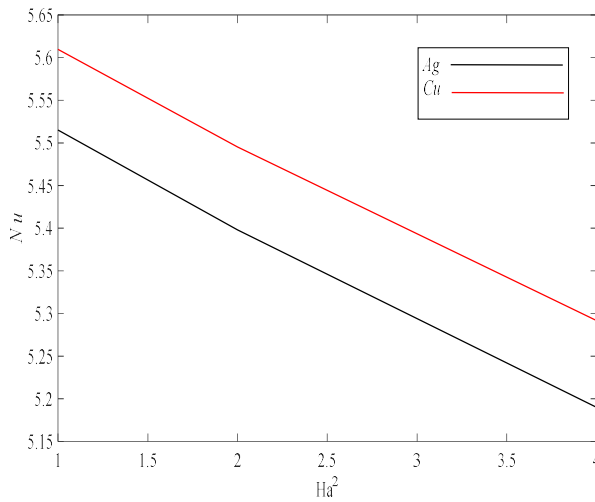


Fig. 22. Comparison of Nusselt number for Ag-H₂O and Cu-H₂O nanofluid w. r. t. Ha²

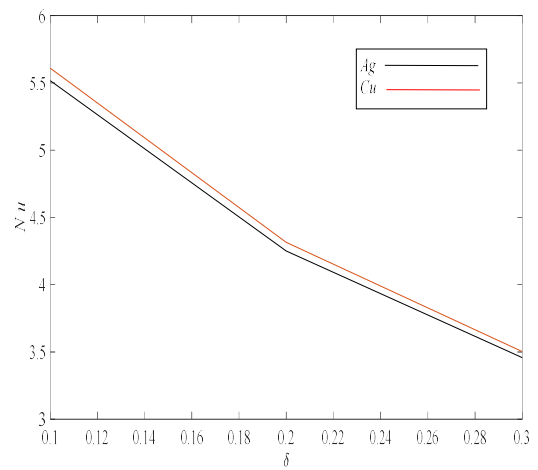


Fig. 23. Comparison of Nusselt number for Ag-H₂O and Cu-H₂O nanofluid w. r. t. delta

Table 2. Comparison of numerous values of $(-\theta'(1))$ with several values of Prandtl number for $\phi=0$, when $Re=10, \gamma=(\pi/2), \lambda = \delta = Ha^2 = Ec = Q = R = K = D = S = 0$:

Pr	Wang [30]	Ahmed et al. [1]	Mishra & Kumar [17]	Present study
0.7	1.568	1.58679	1.586790	1.586790
7.0	6.160	6.15776	6.155812	6.155812

Table 3 displays variation in Nusselt number for different numerical values of the parameters used in the current study. By analyzing Table 3, we demonstrate that the Nusselt number for *Ag*-water and *Cu*-water nanofluids retards for increasing value of parameters K , Ha^2 , R , Q and δ , while opposite trend is found for the parameters D and Re . The above results can also be verified by Figs. 17-23. In addition, we elucidate by referring Figs. 17-23 that heat transfer rate for *Cu*- H_2O nanofluid is higher than *Ag*- H_2O nanofluid always.

Table 3. Numerical values of Nusselt number (Nu), when $Ec=0.3$, $S=0.1$, $\lambda=0.2$, $\phi=0.05$ and $\gamma=\pi/4$

K	$Ha^2 \times 10^{-8}$	δ	D	R	Re	Q	$Nu(Cu)$	$Nu(Ag)$
0.0	1.0	0.1	0.1	0.1	5.0	0.5	5.764110	5.664443
1.0	1.0	0.1	0.1	0.1	5.0	0.5	5.609841	5.515259
4.0							5.251337	5.166946
1.0	2.0	0.1	0.1	0.1	5.0	0.5	5.495331	5.397851
	4.0						5.291876	5.190060
1.0	1.0	0.2	0.1	0.1	5.0	0.5	4.313732	4.251058
		0.3					3.504193	3.458411
1.0	1.0	0.1	2.0	0.1	5.0	0.5	5.655733	5.611874
			5.0				5.826665	5.739297
1.0	1.0	0.1	0.1	0.0	5.0	0.5	6.015532	5.919324
				0.2			5.252656	5.159656
1.0	1.0	0.1	0.1	0.1	6.0	0.5	6.283525	6.186564
					7.0		6.885073	6.786152
1.0	1.0	0.1	0.1	0.1	5.0	-2.0	6.051172	5.969058
						2.0	5.305144	5.200377

CONCLUSIONS

In this article, we analyze and study the behavior of mixed convection boundary layer *MHD* flow of nanofluid (*Ag* / *Cu*- H_2O) through porous stretching inclined cylinder in the presence of thermal radiation. Runge-Kutta fourth order method with shooting technique in *MATLAB* has been taken in to account to acquire solution of non-linear *ODE*'s with associated boundary conditions. Some major conclusions are summarized as follows:

- *Ag*-water and *Cu*-water nanofluid velocity decreases with enhancement in the permeability parameter and suction/injection parameter.
- On accelerating the values of Reynolds number and suction/injection parameters, thermal boundary layer of *Ag*-water and *Cu*-water nanofluid decelerates.
- Nusselt number reduces with increasing values of permeability parameter, heat generation/absorption parameter and radiation absorption parameter but it is proportional to mixed convection parameter and Reynolds number for both *Ag*-water and *Cu*-water nanofluids.
- A larger Nusselt number corresponds to more active convection; here *Cu*-water nanofluid is more convective than *Ag*-water nanofluid.

REFERENCES

- [1] Ahmed, S.E., Hussein, A.K., Mohammed, H.A., Sivasankaran, S., Boundary layer flow and heat transfer due to permeable stretching tube in the presence of heat source/sink utilizing nanofluids, *Appl. Math. Comput.* 238(2014), 149–162.
- [2] Ashorynejad, H. R., Sheikholeslami, M., Pop, I., Ganji, D. D., Nanofluid flow and heat transfer due to a stretching cylinder in the presence of magnetic field, *Heat Mass Transf.*, 49(3) (2013), 427–436.
- [3] Butt, A.S., Ali, A., Mehmood, A., Numerical investigation of magnetic field effects on entropy generation in viscous flow over a stretching cylinder embedded in a porous medium, *Energy*, 99 (2016), 237–249.
- [4] Choi, S.U.S., Enhancing Thermal Conductivity of Fluids with Nanoparticles, *ASME Publications-Fed*, 231(1995), 99–106.
- [5] Ganga, B., Ansari, S.M.Y., Ganesh, N.V., Hakeem, A.A., *MHD* radiative boundary layer flow of nanofluid past a vertical plate with internal heat generation/absorption, viscous and ohmic dissipation effects, *J. Nigerian Math. Soc.*, 34 (2) (2015), 181–194.
- [6] Hakeem, A. K., Ganesh, N. V., Ganga, B., Magnetic field effect on second order slip flow of nanofluid over a stretching/shrinking sheet with thermal radiation effect, *J. Magn. Magn. Mater.*, 381(2015), 243–257.
- [7] Hayat, T., Imtiaz, M., Alsaedi, A., Melting heat transfer in the *MHD* flow of *Cu*-water nanofluid with viscous dissipation and Joule heating, *Adv. Powder Technol.*, 27(4)(2016), 1301–1308.
- [8] Hayat, T., Shafiq, A., Alsaedi, A., *MHD* axisymmetric flow of third grade fluid by a stretching cylinder, *Alexandria Eng. J.*, 54(2) (2015), 205–212.
- [9] Hayat, T., Shafique, M., Tanveer, A., Alsaedi, A., Magnetohydrodynamic effects on peristaltic flow of hyperbolic tangent nanofluid with slip conditions and Joule heating in an inclined channel, *Int. J. Heat Mass Transf.* 102(2016), 54–63.
- [10] Hussain, A., Malik, M.Y., Salahuddin, T., Bilal, S., Awais, M., Combined effects of viscous dissipation and Joule heating on *MHD* Sisko nanofluid over a stretching cylinder, *J. Mol. Liq.*, 231 (2017), 341–352.
- [11] Ishak, A., Nazar, R., Pop, I., Uniform suction/blowing effect on flow and heat transfer due to a stretching cylinder, *Appl. Math. Model.*, 32 (10) (2008), 2059–2066.
- [12] Ishak, A.M., Nazar, R.M., Laminar boundary layer flow along a stretching cylinder, *Eur. J. Sci. Res.*, 36 (1) (2009), 22–29.
- [13] M. Khan, R. Malik, A. Munir, W.A. Khan, Flow and heat transfer to Sisko nanofluid over a nonlinear stretching sheet, *PLoS ONE*, 10 (5) (2015).

- [14] Majeed, A., Javed, T., Ghaffari, A., Rashidi, M.M., Analysis of heat transfer due to stretching cylinder with partial slip and prescribed heat flux: a Chebyshev spectral Newton iterative scheme, *Alexandria Eng. J.*, 54(4)(2015), 1029–1036.
- [15] Malik, R., Khan, M., Mushtaq, M., Cattaneo-Christov heat flux model for Sisko fluid flow past a permeable non-linearly stretching cylinder, *J. Mol. Liq.* 222 (2016), 430–434.
- [16] Mishra, A. and Kumar, M., Ohmic-viscous dissipation and heat generation/absorption effect on MHD nanofluid flow over a stretching cylinder with suction/injection, *Adv. Compu. Commu. Tech.*, 702(2019).
- [17] Mishra, A., Pandey, A.K., Chamkha, A.J., Kumar, M., Roles of nanoparticles and heat generation/absorption on MHD flow of Ag–H₂O nanofluid via porous stretching/shrinking convergent/divergent channel, *J. Egypt. Math. Soc.*, 28(2020), 1–18.
- [18] Mishra, A., Pandey, A.K., Kumar, M., Ohmic-viscous dissipation and slip effects on nanofluid flow over a stretching cylinder with suction/injection, *Nanosci. Technol. Int. J.*, 9(2)(2018), 99–115.
- [19] Mishra, A., Pandey, A.K., Kumar, M., Velocity, thermal and concentration slip effects on MHD silver–water nanofluid flow past a permeable cone with suction/injection and viscous-Ohmic dissipation, *Heat Transf. Res.* 50(14)(2019), 1351–1367.
- [20] Mukhopadhyay, S., MHD boundary layer slip flow along a stretching cylinder, *Ain Shams Eng. J.*, 4(2) (2013), 317–324.
- [21] Naramgari, S. and Sulochana, C., MHD flow of dusty nanofluid over a stretching surface with volume fraction of dust particles, *Ain Shams Eng. J.*, 7 (2) (2016), 709–716.
- [22] Pal, D., Mandal, G., Vajravelu, K., Flow and heat transfer of nanofluids at a stagnation point flow over a stretching/shrinking surface in a porous medium with thermal radiation, *Appl. Math. Comput.*, 238(2014), 208–224.
- [23] Pandey, A.K., Kumar, M., Natural convection and thermal radiation influence on nanofluid flow over a stretching cylinder in a porous medium with viscous dissipation, *Alexandria Eng. J.*, 56(1)(2017), 55–62.
- [24] Pandey, A.K., Kumar, M., Boundary layer flow and heat transfer analysis on Cu–water nanofluid flow over a stretching cylinder with slip, *Alex. Eng. J.*, 56(4) (2017), 671–677.
- [25] Pandey, A.K., Kumar, M., MHD flow inside a stretching/shrinking convergent/divergent channel with heat generation/ absorption and viscous-Ohmic dissipation utilizing Cu–water nanofluid, *Comput. Therm. Sci. Int. J.*, 10(5)(2018), 457–471.
- [26] Singh, K., Pandey, A. K., Kumar, M., Melting heat transfer assessment on magnetic nanofluid flow past a porous stretching cylinder, *J. Egypt. Math. Soc.*, 29 (2021), 1.
- [27] Wang, C.Y., Fluid flow due to a stretching cylinder, *Phys. Fluid.*, 31(3) (1988), 466–468.
